Journal of Electronic Materials (2023) 52:2158–2167
https://doi.org/10.1007/s11664-022-10183-y

ORIGINAL RESEARCH ARTICLE

Enhanced Proton Conductivity of a Sulfonated Polyether Sulfone Octyl Sulfonamide Membrane via the Incorporation of Protonated Montmorillonite

Walid Mabrouk[1] · Khaled Charradi[2] · Ahmed Mellekh[3] · Amor Hafiane[1] · Qana A. Alsulami[4] · Hager M. Meherzi[5] · Radhouane Chtourou[2] · Sherif M. A. S. Keshk[2]

Received: 12 June 2022 / Accepted: 19 December 2022 / Published online: 9 January 2023

Abstract

Hybrid membranes consisting of sulfonated poly (ether sulfone) octyl sulfonamide (SPESOS) cast together with protonated montmorillonite (H-MMT, 1, 3, and 6 wt%) were fabricated and characterized. Fourier-transform infrared (FT-IR) spectra of the H-MMT/SPESOS composites confirmed that no chemical reactions occurred between the SPESOS and clay. X-ray diffractograms (XRD) showed a significant shift in the major peak of SPESOS at $2\theta = 15.5°$ due to the incorporation of H-MMT. Furthermore, scanning electron microscopy (SEM) confirmed a homogeneous structure of the composite, and thermogravimetric analysis (TGA) results revealed that the addition of H-MMT promoted water absorption via the decrease in the loss of composite mass during evaporation. The SPESOS with H-MMT had higher water retention, contact angle, and proton conductivity values than pristine SPESOS. The proton conductivity of the hybrid membranes, however, improved at 100°C from 42 mS/cm in pure SPESOS to 787, 350, and 300 mS/cm for the 1, 3, and 6 wt% H-MMT hybrids, respectively. These results demonstrate that the incorporation of the H-MMT is a viable strategy to boost the performance of SPESOS to construct a possible membrane for applying in fuel cells.

Keywords SPESOS · proton conductivity · protonated montmorillonite · composite membrane · fuel cells

Abbreviations

SPESOS	Sulfonated poly ether sulfone octyl sulfonamide
H-MMT	Protonated montmorillonite
MMT	Montmorillonite
DMFC	Direct methanol fuel cell
PEM	Proton exchange membrane
SPES	Sulfonated poly ether sulfone
PEO	Poly ethylene oxide
SPEEK	Sulfonated poly ether ether ketone
PBI	Polybenzimidazole
SiO_4	Silica tetrahedral layer
Al_2O_6	Alumina octahedral layer
H_2SO_4	Sulfuric acid
NaOH	Sodium hydroxide
FT-IR	Fourier-transform infrared spectroscopy
XRD	X-ray diffraction
TGA	Thermogravimetric analysis
SEM	Scanning electron microscopy
WU	Water uptake
CA	Contact angle
IEC	Ion exchange capacity
DS	Degree of sulfonation
RH	Relative humidity
E_a	Activation energy

✉ Walid Mabrouk
w.mabroukcerte@gmail.com

1 Laboratory Water, Membranes and Biotechnology of the Environment, CERTE, 8020 Soliman, Tunisia

2 CRTEn, Nanomaterials and Systems for Renewable Energy Laboratory, Research and Technology Center of Energy, Technopark Borj Cedria, BP 095 Hammam Lif, Tunisia

3 FSB, Chemistry Laboratory of Materials, LR13ES08, University of Carthage, Jarzouna, 7021 Bizerta, Tunisia

4 Chemistry Department, Faculty of Science, King Abdulaziz University, Jeddah 21589, Saudi Arabia

5 FST, Laboratory of Analytical Chemistry and Electrochemistry, LR99ES15, University of Tunis El Manar, Campus, 2092 Tunis, Tunisia

Introduction

Fuel cells play a key role in the efforts to relieve global warming and decrease the reliance on fossil fuels. Among the available types of fuel cells, direct methanol fuel cells (DMFCs) have particular advantages in applications such as electronic devices and transportation, as they exhibit high energy density at low temperatures, and their fuel source (methanol) is relatively easy to store and handle.[1] A key element of any DMFC is the proton-exchange membrane (PEM), which acts as a barrier separating the anode and cathode reactants while still permitting protons to move between the electrodes while the cell is in use. Additionally, the PEM has high oxidative and hydrolytic stability, great mechanical durability in both dry and hydrated states, and low operating costs in practical fuel cells.[2] Sulfonated poly (ether sulfone) (SPES) has been investigated extensively as an alternative to Nafion as the material of choice for PEM, due to its thermo-mechanical, oxidative, and chemical stability.[3] SPES can also be effectively functionalized. In our previous study, we proposed grafting pending chains of octylamine within sulfonated poly (arylene ether sulfone) (SPES), an approach that retains the polyaromatic skeleton of PES.[4] The composite that resulted was sulfonated polyether sulfone octyl sulfonamide (SPESOS), which showed an ionic exchange capacity (IEC) of two mEq/g (1 H^+ per monomer unit), useful levels of ionic conductivity, and a proton transport number close to one.[4,5] Clays have also been investigated as a possible additive to conductive polymers.[6] Clay/polymer composite membranes might possess extra dimensional stability and, therefore, stronger polymer/electrode interfaces, which can enhance the durability of fuel cells.[7] These enhancements probably arise due to the interaction between the polymer (organic matrix) and clay (an inorganic matrix) at a molecular level.[8] Clay minerals can also act as electrical conductors. Clays that have silicates, alumina, and metal cations in their main structure increase proton conductivity and impart high mechanical stability.[9]

The silicates, alumina, and metal cations form separate layers within the clays, and different clays have layers with different ratios of silicates to alumina.[10] Several studies on the use of silica as an inorganic additive to PEM have concluded that the physical characteristics of the resulting hybrid materials have a great impact on the durability, water retention ability, and fuel permeability of the membrane.[11] One clay that is an effective additive is the naturally occurring MMT, which belongs to the class of clay minerals that consist of three layers, including a silica tetrahedral layer (SiO_4), an alumina octahedral layer (Al_2O_6), and an exchangeable cation layer.[12] Thus, MMT not only influences the electrochemical characteristics of the ion exchange membrane, such as ion conductivity and permeability, but also its thermal and mechanical stability, which is a great advantage for applications such as reverse osmosis, ultra-filtration, pervaporation, gas separation, and DMFCs.[13–17] The intercalated or exfoliated MMT in MMT–polymer composites plays a key role in ionic conduction in the electrolytes.[18–25] The electronic conductivity of MMT–polyaniline composite materials significantly increases with an increase in the quantity of polyaniline within the interlayer space.[26] A Nafion–MMT-hybridized membrane is a promising alternative to pure Nafion, displaying proton conductivities of up to 38.5 mS/cm and an ethanol permeability of below 0.69×10^{-6} cm^2/s.[27] MMT was also combined with polyethylene oxide (PEO) with the polysaccharide chitosan as a secondary filler. The MMT hybrid membranes displayed promising PEM features, such as good proton conductivity (2.99×10^{-2} S/cm at room temperature), acceptable ion exchange capacity (2.84 mEq/g), low swelling ratio (21%), and useful water uptake (55.7%).[28] The hybrid contained 15% wt% of MMT functionalized with protons (H^+-MMT), while the PEO content was 85 wt% of the polymer chains, indicating that much less MMT than PEO was needed to improve membrane performance.[21] MMT and chitosan have also been combined with sulfonated poly (ether ether ketone) (SPEEK).

A study on the performance of SPEEK incorporated with Mg_2Al-layered double hydroxide (Mg–Al LDH) and SiO_2-MMT improved SPEEK, and showed that the composite membranes displayed better proton conductivity (0.070 S/cm and 0.158 S/cm, respectively) compared to a pure SPEEK membrane (0.023 S/cm) at 120°C.[29] Incorporating MMT within a SPESOS matrix showed a considerable increase in proton conductivity (485 mS/cm) over the pure SPESOS (42 mS/cm), which might be attributed to an increase in the hydrophilicity of the membrane by about 25%.[30] The use of a H-MMT-incorporated polymer matrix has gained much attention and can further enhance the electrochemical properties of the membranes.[31–33] Polybenzimidazole (PBI) membranes doped with phosphoric acid and containing high levels of H-MMT showed a significant increase in proton conductivity and mechanical properties.[34] This can be attributed to the water trapped in the H-MMT channels acting as a water reservoir in the composite membrane, with the enhancement being more pronounced as the H-MMT content was reduced. This latter study suggested that A H-MMT filler is a promising high-performance PEM candidate for fuel cell applications.[35,36] Numerous studies have been carried out on the behavior of membrane proton conductivity at high temperatures. For instance, SPEEK with 1 wt% MMT at 100°C had a conductivity of 105 mS/cm. The conductivity of protonated MMT-elaborated membrane was significantly higher than that of composite membranes made

with the same mass percentages of non-protonated montmorillonite mentioned in a prior study. The membrane containing 1% by weight of MMT had a proton conductivity of 468 mS/cm, while the membrane containing 1% by weight of H-MMT had a proton conductivity of 787 mS/cm.[36]

In this study, SPESOS and H-MMT hybrid membranes with better electrochemical and thermal performance were synthesized and evaluated. The IEC, water uptake, and proton conductivity of the fabricated composite membranes were used to investigate their suitability for usage in DMFCs.

Materials and Methods

Materials

The SPESOS base material was synthesized by the authors[1] at Eras Labo (Saint-Nazaire-Les-Eymes, France).[4] Analytical grade reagents were purchased from Acros (N,N'-dimethylacetamide), Schlarlau (sulfuric acid, H_2SO_4), and Laurylab (sodium hydroxide, NaOH).

Preparation of Protonated Montmorillonite

MMT is a soft phyllosilicate mineral of the smectic group with the chemical formula $(Na, Ca)_{0.33}(Al, Mg)_2Si_4O_{10}(OH)_2$ nH_2O. H-MMT was synthesized by adding MMT to 1 M H_2SO_4 and stirring for 24 h. The resulting slurry was filtered to separate H-MMT as a white powder. The structure of H-MMT is shown in Fig. 1.

Composite Membrane Preparation

Three H-MMT/SPESOS composite solutions, consisting of SPESOS incorporated with either 1, 3, or 6 wt% of H-MMT solid filler, were prepared by mixing the raw ingredients in dimethylacetamide (30 wt%), followed by sonicating at ambient temperature for 2 h. Composite membrane products were then fabricated by casting each composite solution onto a Teflon substrate (surface = 100 cm^2), followed by heat treatment in an oven at a range of temperatures.[37,38]

Experimental

Characterization

Fourier-transform infrared (FT-IR) spectra of SPESOS and the different composite membranes were acquired across the range of 400–4000 cm^{-1} using a Nicolet spectrophotometer (IR200 FT-IR) operating in transmission mode. The x-ray diffraction (XRD) patterns of the dry hybrid membranes were acquired using a Bruker D8 Advance x-Ray Diffractometer with 2θ between 5° and 60°. Thermogravimetric analysis (TGA) of the polymer samples was performed on a Mettle TGA thermogram. Before performing TGA, samples weighing between 2.5 and 3.5 mg were vacuum-dried at 100°C for 24 h to remove residual solvents. TGA curves were recorded across a range

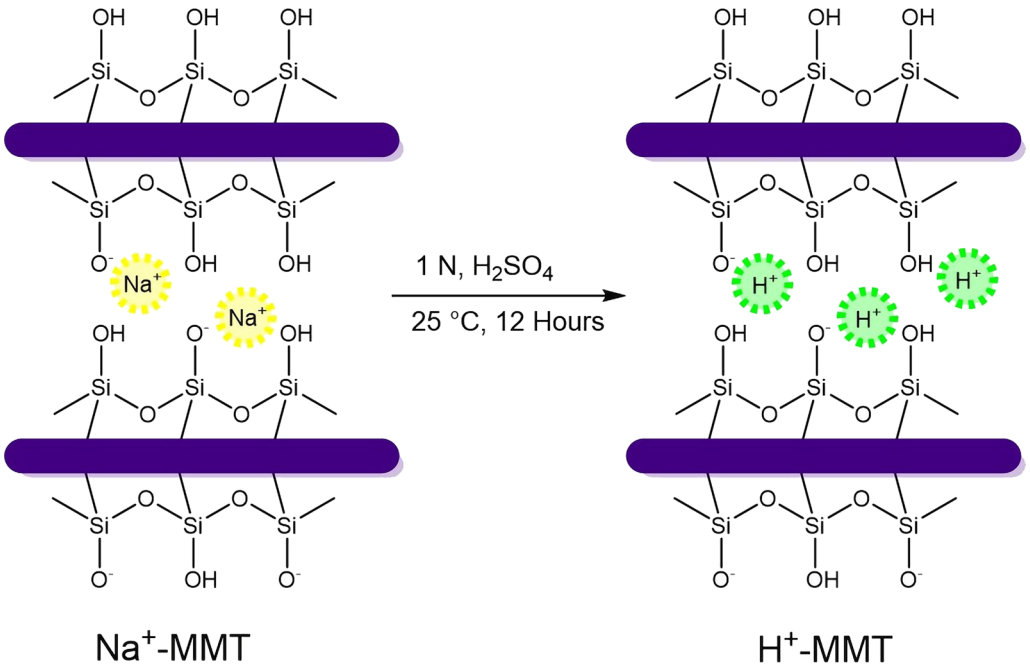

Fig. 1 Structure of the base (Na^+-MMT) and protonated montmorillonite (H-MMT).

of temperatures (from ambient to 700°C). Scanning electron microscopy (SEM; Hitachi 4800 II) was used to characterize the surfaces and cross-sections of the membranes. For the latter observation, the membranes were first fractured after cooling with liquid nitrogen. Observations were made without any prior treatment of the samples. The degree of water uptake (WU) at room temperature was determined by first soaking the dry membrane in distilled water for two days, followed by weighing the membrane after removing the water using paper. [39] The WU values were calculated from the difference in mass before and after swelling of the membrane by water according to Eq. 1:

$$\mathrm{WU} = \frac{W_{\mathrm{wet}} - W_{\mathrm{dry}}}{W_{\mathrm{dry}}} \times 100 \tag{1}$$

where W_{wet} and W_{dry} are the weights of the wet and dry membranes, respectively.

The water contact angle (CA) was measured with an Attension Theta optical tensiometer (Biolin Scientific) using samples of the different membranes cut into 1.5 cm × 1.5 cm pieces. In each measurement, a deionized water droplet of 5 µL was immobilized on the surface of the membrane using a micro-syringe. Then, a light source was placed behind the sample, and an image of the drop of water was taken using a camera. The contact angle was calculated using the Theta Attension computer software (Biolin).

The ionic exchange capacity (IEC) of a membrane is the measure of the number of ionic sites per monomer unit of dry mass (mEq/g). This measure is widely used to compare different polymers. To determine this, the proton exchange membrane ($S = 5 \times 5$ cm^2) is immersed in a 10^{-2} -M NaOH solution for 48 h, and all the H^+ ions present in the membrane are neutralized by the OH^- ions of the basic solution. The IEC is determined by evaluating the concentration of sodium hydroxide solution remaining following the exchange.[40] The IEC for each membrane is the mEq of sulfonic groups/g of dry polymer and is defined by Eq. 2:

$$\mathrm{IEC} = \frac{n^{I}_{\mathrm{NaOH}} - n^{f}_{\mathrm{NaOH}}}{W_{\mathrm{dry}}} \tag{2}$$

where $n^{\mathrm{I}}_{\mathrm{NaOH}}$ is the initial mol amount of sodium hydroxide in the solution (10^{-2} M, 200 mL), $n^{\mathrm{f}}_{\mathrm{NaOH}}$ is the mol amount of sodium hydroxide after the exchange, and W_{dry} is the dry mass of the membrane.

The IEC value was used to determine the degree of sulfonation (DS) of the different prepared membranes according to Eq. 3;

$$\mathrm{DS} = \frac{M_2 \times \mathrm{CEI}}{1000 + \left(M_2 - M_1\right) \times \mathrm{CEI}} \tag{3}$$

where CEI is the IEC, and M_1 and M_2 are the molar masses of the SPESOS (591.02 g/mol) and the PES (442.53 g/mol), respectively.[41]

Electrochemical impedance spectroscopy was performed using a VSP potentiostat (Biologic Science Instruments) to determine the intrinsic ionic conductivity of the membranes at a range of temperature and 100% relative humidity (RH). The membranes were cut into disc-shaped samples and placed between two platinized blocking electrodes. A frequency response analysis was performed by plotting high-frequency Nyquist plots from data captured by sweeping the frequency between 1000 kHz and 10 Hz with an oscillating voltage amplitude of 10 mV. The electrical resistance (R) was determined from the intersection of the high-frequency arc and the axis of real Zr. The ionic conductivity (σ, S/cm) was calculated according to Eq. 4:

$$\sigma(\mathrm{mS/cm}) = \frac{e}{RxS} \tag{4}$$

wher e is the thickness, S is the surface area of the membrane laid between the two electrodes, and R is its electrical resistance.

Results and Discussion

FT-IR spectra of the composite membranes and the base materials are shown in Fig. 2.

The spectrum of H-MMT showed bands at 3626 cm^{-1} and 1630 cm^{-1} (Fig. 2a), corresponding to stretching and bending of O-H, respectively, while the bands at 1042 cm^{-1} and 1120 cm^{-1} could be assigned to Si-O and

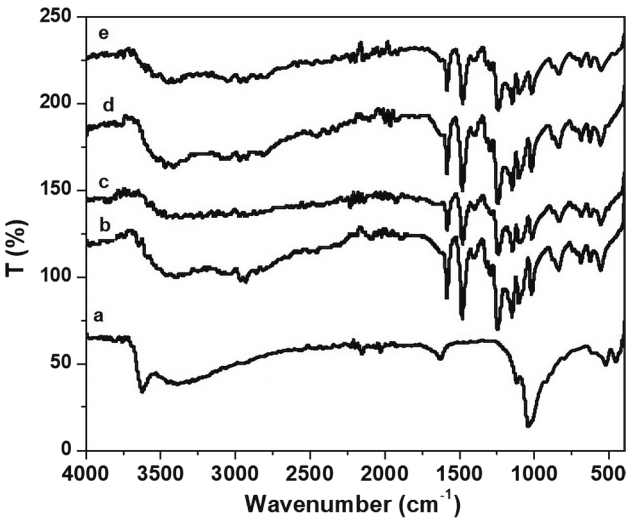

Fig. 2 FT-IR spectra for (a) H-MMT (a), (b) SPESOS, (c) 1% H-MMT/SPESOS, (d) 3% H-MMT/SPESOS, and (e) 6% H-MMT/SPESOS.

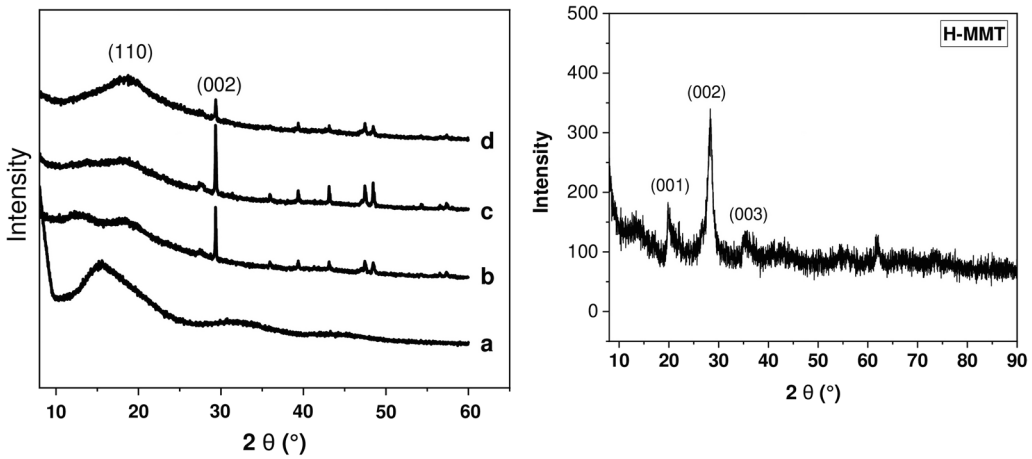

Fig. 3 X-ray diffraction patterns of (a) SPESOS, (b) 1% H-MMT/SPESOS, (c) 3% H-/SPESOS, and (d) 6% H-MMT/SPESOS and H-MMT.

Al-O stretching modes, respectively, showing that the core structure of MMT remained after the surface amendment by sulfuric acid. The spectrum of SPESOS (Fig. 2b) showed bands at 1482 cm^{-1} and 1590 cm^{-1}, corresponding to the aromatic carbons, and at 1005 cm^{-1} and 1074 cm^{-1}, corresponding to O=S=O.

The spectra of the H-MMT/SPESOS composites (Fig. 2(c–e)) showed no significant difference irrespective of the quantity of added H-MMT (1 wt%, 3 wt%, or 6 wt%), showing that no chemical reactions occurred between the SPESOS and clay.

XRD was used to inspect the dispersal of the H-MMT platelet stacks in the SPESOS chains. The XRD pattern of the latter revealed an amorphous structure with a major peak at $2\theta = 15.5°$ that was assigned to the (110) plane, whereas the pattern of H-MMT showed three characteristic peaks at $2\theta = 6.79°$, 19.91°, and 28.22° corresponding to (001), (002) and (003), respectively (Fig. 3).

The SPESOS membrane composites showed a significant shift in the major peak of SPESOS from $2\theta = 15.5°$ to 18.7° in the three composites.

This shift was due to the incorporation of H-MMT, resulting in poor macromolecular orientations of the SPESOS chains. Thus, increasing the quantity of the incorporated H-MMT increased the degrees of interaction between H-MMT and SPESOS.

These results suggested that the H-MMT layers were intercalated, exfoliated, and dispersed in the SPESOS matrix. The crystallite size also decreased with an increase in the quantity of H-MMT, as shown in Table I.

This result showed that there was a marked loss of crystallinity due to the incorporation of H-MMT clay onto the SPESOS matrix, suggesting that high proton conductivity might be possible.

Table I Results of the XRD analysis of SPESOS and its H-MMT composites

Sample	2θ (°) (110)	Mean crystallite size (nm)
SPESOS	15.40	5.89
1% H-MMT/SPESOS	18.21	4.80
3% H-MMT/SPESOS	18.30	4.75
6% H-MMT/SPESOS	18.50	4.65

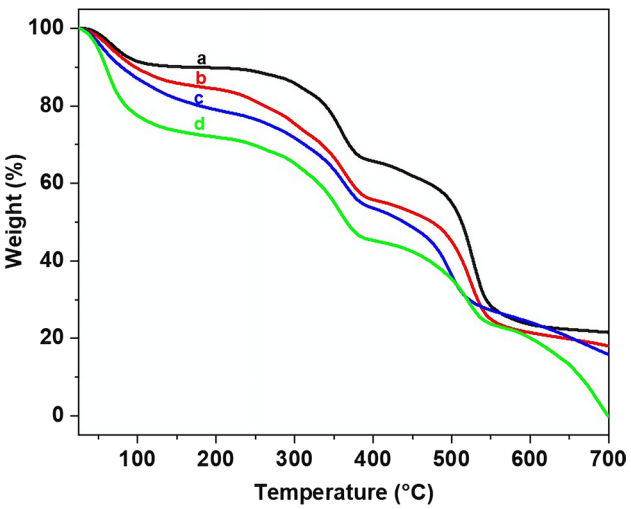

Fig. 4 Thermogravimetric analysis of (a) SPESOS, (b) 1% H-MMT/SPESOS, (c) 3% H-/SPESOS, and (d) 6% H-MMT/SPESOS.

The thermal stability of the hybrid membranes and the pure SPESOS membrane, determined via TGA analysis, is shown in Fig. 4.

The thermograms were very similar in appearance (Fig. 4), presenting the same stages of mass loss corresponding to the vaporization of water at around 100°C, followed by a second significant loss of mass, which occurred at around 300°C and might be due to the deterioration of the sulfonated groups with the release of SO_2 and H_2O.[37]

The final mass loss was observed at around 500°C, and can be ascribed to the degradation of the backbone of the macromolecular chain of the base polymer. The most important observation was that the loss of mass during the evaporation of water decreased as the percentage of H-MMT increased, which indicated that the addition of H-MMT can promote water absorption. The analysis also indicated that the thermal stability of all the hybrid membranes is acceptable at the temperatures corresponding to fuel cell applications.

Scanning electron microscopy (SEM) was used to examine the morphological structure of the hybrid membranes as an indication of the electrochemical properties that are associated with their microstructure, such as the spatial dispersion of their ionic sites. The SEM images showed that the composite membranes had a homogeneous structure free from cracks, holes, and pores (Fig. 5).

These results showed that the in situ polymerization method could be used to prepare proton exchange films containing different ratios of H-MMT and SPESOS distributed uniformly.

The two main determinants of the electrochemical behavior of hybrid membranes are water uptake and IEC. The IEC is the number of milli-equivalents of ions in 1 g of SPESOS (mEq/g). An IEC of 2.84 mEq/g was detected for 0.3 equivalents of octylamine with pure sulfo-chlorinated poly (ether sulfone). The left one, SO_2Cl group per monomer unit, in the free state that could be transformed by hydrolysis into an SO_3H group through acid–base titration. The results of the IEC analysis are shown in Table II.

The results showed that the SPESOS reference membrane provided the lowest IEC (2 mEq/g), while the incorporation of H-MMT in the SPESOS membrane increased its exchange capacity, because the protons that were provided by the clay increased the interactions between the H-MMT and the SO_3H groups of the SPESOS. The increase in proton transfer made these hybrid membranes attractive for use as PEM in fuel cells.

The water contact angle of a membrane surface correlates strongly with the hydrophobicity or hydrophilicity of the membrane. The observed contact angle values for SPESOS and the composites membranes are shown in Fig. 6.

The water contact angle of all the composites membranes was below 80° (Fig. 6). The increase in the polarity of the hybrid membranes due to the incorporation of H-MMT

Table II IEC of all the membranes

Membrane	Ion exchange capacity (mEq/g)
SPESOS	1.91
1% H-MMT/SPESOS	2.15
3% H-MMT/SPESOS	2.29
6% H-MMT/SPESOS	2.35

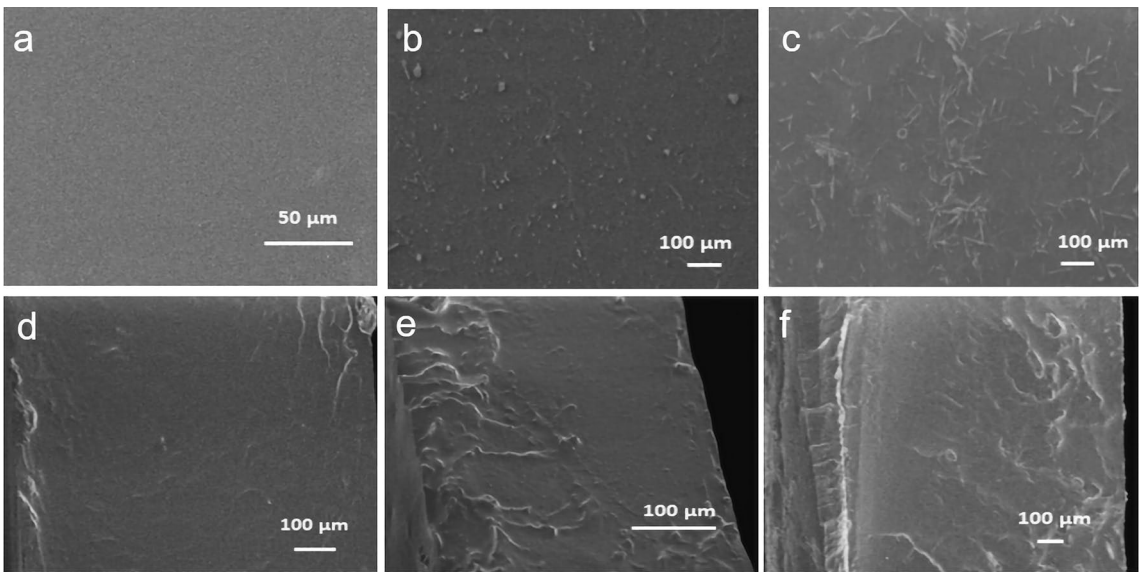

Fig. 5 SEM images of the membrane surfaces: (a) SPESOS, (b) 1% H-MMT/SPESOS, (c) 3% H-/SPESOS, and (d) 6% H-MMT/SPESOS. Cross-section (d) 1% H-MMT/SPESOS, (e) 3% H-MMT/SPESOS, and (f) 6% H-MMT/SPESOS.

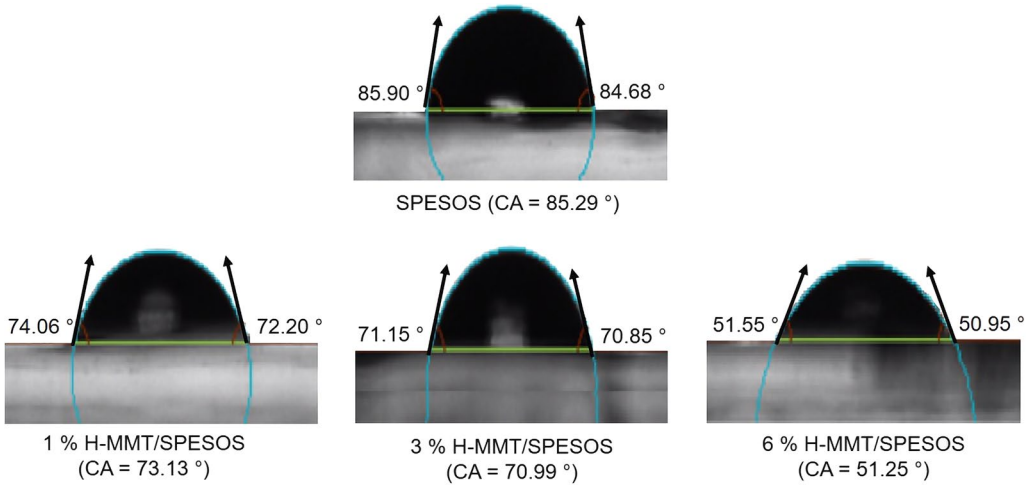

Fig. 6 Results of the contact angle measurements for SPESOS and the composite membranes.

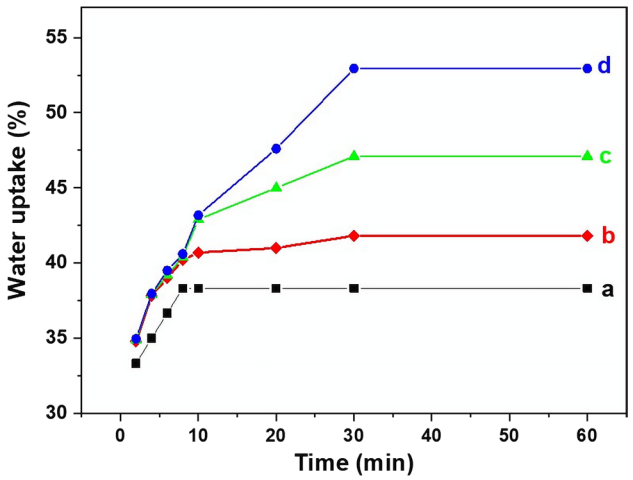

Fig. 7 Water uptake of all membranes after 1 h: (a) SPESOS, (b) 1% H-MMT/SPESOS, (c) 3% H-/SPESOS, and (d) 6% H-MMT/SPESOS.

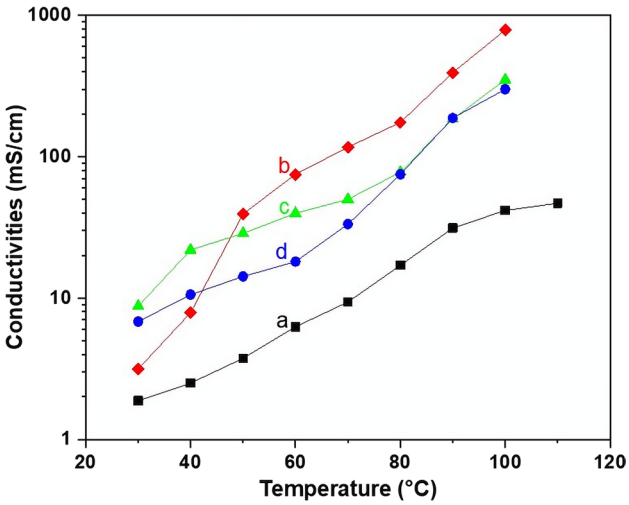

Fig. 8 Proton conductivity at 100% RH of the (a) SPESOS, (b) 1% H-MMT/SPESOS, (c) 3% H-/SPESOS, and (d) 6% H-MMT/SPESOS.

increased the affinity for water, permitting more water uptake without excess swelling that would adversely affect the performance of the membrane in a fuel cell.

This further supported the argument that these membranes are good candidates for being used as PEM within fuel cells. Water uptake is a key requirement in determining the properties of SPESOS membranes. Ionic membranes are bad proton conductors in the dry state, only becoming conductive once hydrated. The water uptake of the hybrid H-MMT/SPESOS membranes was evaluated by monitoring the changes in weight between the dry and hydrated membranes. The results are shown in Fig. 7.

The pristine SPESOS membrane contains few polar functional groups, only SO_3H, and thus, displayed a low water-attracting capacity, as found from its high contact angle (85.29°). Water uptake changed considerably when H-MMT was incorporated into the SPESOS, due to the hydrophilic nature of the H-MMT clay filler and their chemical compatibility. This increased water uptake and promoted the formation of large areas within the membrane with ionic groups that permitted the exchange of protons via the conduction channels without any hindrance. There was no significant change in the water uptake by the various hybrid membranes after 48 h. These results again supported the argument that the new hybrid membranes with H-MMT would function as a good PEM in fuel cells.

Proton conductivity is the most significant property of hybrid membranes when used in electrolysis. The proton

Table III Activation energies and protonic conductivities at 100°C for pure SPESOS and the composite membranes

Membrane	Conductivity (mS/cm) at 100°C	E_a (kJ/mol)
SPESOS	42	38.1
1% H-MMT/SPESOS	787	23.2
3% H-MMT/SPESOS	350	25.3
6% H-MMT/SPESOS	300	28.2

conductivity spectra of the membranes at a range of temperatures are shown in Fig. 8.

The hybrid membranes showed higher proton conductivity than pure SPESOS at all temperatures, which might be attributed to the improved IEC and water uptake described above, probably due to the protons contributed by the H-MMT. At low temperatures, the protonic conductivity of the composite membranes was low. However, at 100°C, the proton conductivity of the hybrid membranes increased from 42 mS/cm in pure SPESOS to 787 mS/cm, 350 mS/cm, and 300 mS/cm for the 1 wt%, 3 wt%, and 6 wt% H-MMT hybrids, respectively. The proton conductivity (from 50°C) of the composite membranes decreased when the H-MMT loading content increased.

The aggregation of H-MMT, as shown in the SEM images (Fig. 5), might hinder the transfer of protons in the membrane.[32,33]The activation energy (E_a), which is the minimum energy needed for proton transport across the membrane, was calculated from an Arrhenius plot of proton conductivity as a function of temperature at 100% RH based on Eq. 5:

$$\sigma = \sigma_0 \exp(-E_a/\mathrm{RT}) \tag{5}$$

where σ is the proton conductivity (S/cm), σ_0 is the pre-exponential factor, R is the universal gas constant (8.314472 J/mol. K), and T is the absolute temperature (K). As shown in Table III, the composite membranes showed lower Ea values than pure SPESOS, indicating that proton conduction occurred more readily in the composites.

The incorporation of clay influenced the E_a, and the lowest value was obtained for 1 wt% clay, confirming the results obtained for proton conductivity. The increase in E_a with an increase in the percentage of H-MMT might be attributed to the formation of agglomeration or chunks in the SPESOS matrix that hindered proton transfer. The high proton conductivity obtained at 100°C with only 1% clay also confirmed the presence of water in the composite, which allowed the protons to accelerate at high temperatures. These conductivity values were higher than those found in a Nafion membrane with incorporated clay, which was ~ 126 mS/cm^2 at 100°C.[32]

Conclusions

Membranes based on a composite H-MMT/SPESOS structure were fabricated for a range of clay concentrations. We found that the membrane properties, such as contact angle, IEC, water uptake, and protonic conductivity, were strongly related to the concentration of the clay added to the membrane. The addition of H-MMT increased water uptake, IEC, and contact angle, and also increased the efficiency of protonic conduction compared to the values of these parameters for pure SPESOS. The best-performing composite (1% H-MMT/SPESOS) showed conductivity values 1500 times greater than that of pure SPESOS at high temperatures and 100% humidity.

These findings suggest that the H-MMT/SPESOS composite membranes, which possess excellent chemical and physical properties, are promising for their use in proton exchange membrane fuel cells. Reverse osmosis and ultrafiltration, microbial fuel cells, the fabrication of modified electrodes, and other uses are all possible with the synthesized H-MMT/SPESOS composite membranes.

Acknowledgments The authors extend their appreciation to the manager of Eras Labo company for providing the SPESOS polymer free of charge.

Conflict of interest The authors declare that they have no known competing financial interest or personal relationships that could have appeared to influence the work reported in this paper.

References

1. J.C. Cruz, V. Baglio, S. Siracusano, R. Ornelas, L.G. Arriaga, V. Antonucci, and A.S. Arico, Nanosized Pt/IrO_2 electrocatalyst prepared by modified polyol method for application as dual function oxygen electrode in unitized regenerative fuel cells. *Int. J. Hydrog. Energy* 37, 5508 (2012).
2. J. Kim, I. Lee, Y. Tak, B.N. Cho, and S.Y. Nam, State-of-health diagnosis based on hamming neural network using output voltage pattern recognition for a PEM fuel cell. *Int. J. Hydrog. Energy* 37, 4280 (2012).
3. S. Gahlot and V. Kulshrestha, Graphene based polymer electrolyte membranes for electrochemical energy applications. *Int. J. Hydrog. Energy* 45, 17029 (2020).
4. W. Mabrouk, L. Ogier, F. Matoussi, C. Sollogoub, S. Vidal, M. Dachraoui, and J.F. Fauvarque, Preparation of new proton exchange membranes using sulfonated poly(ether sulfone) modified by octylamine (SPESOS). *Mater Chem. Phys.* 128, 456 (2011).
5. W. Mabrouk, L. Ogier, S. Vidal, C. Sollogoub, F. Matoussi, M. Dachraoui, and J.F. Fauvarque, Synthesis and characterization of polymer blends of sulfonated polyethersulfone and sulfonated polyethersulfone octysulfonamide for PEMFC applications. *Fuel Cells* 12, 197 (2012).
6. Z. Ahmed, Q.A. Alsulami, K. Charradi, S.M.A.S. Keshk, and R. Chtourou, Physicochemical characterization of low sulfonated

polyether ether ketone/smectite clay composite for proton exchange membrane fuel cell. *J Appl. Polym. Sci.* 138, 49634 (2021).
7. K. Charradi, Z. Ahmed, N. Thmaini, P. Aranda, Y.O. Al-Ghamdi, P. Ocon, S.M.A.S. Keshk, and R. Chtourou, Incorporation of layered double hydroxide/sepiolite to improve the performance of sulfonated poly(ether ether ketone) composite membranes for proton exchange membrane fuel cells. *J. Appl. Polym. Sci.* 138, e50364 (2021).
8. N.A.M. Harun, N. Shaari, and N.F.H.N. Zaiman, A review of alternative polymer electrolyte membrane for fuel cell application based on sulfonated poly(ether ether ketone). *Int. J. Energy. Res.* 45, 1 (2021).
9. D. Xing, G. He, Z. Hou, P. Ming, and S. Song, Preparation and characterization of a modified montmorillonite/sulfonated polyphenylether sulfone/PTFE composite membrane. *Int. J. Hydrog. Energy* 36, 2177 (2011).
10. T.V. Shapley, M. Molinari, R. Zhu, and S.C. Parker, Atomistic modeling of the sorption free energy of dioxins at clay-water interface. *J. Phys. Chem.* 117, 24975 (2013).
11. Y.P. Ying, S.K. Kamarudin, and M.S. Masdar, Silica-related membranes in fuel cell applications: an overview. *Int. J. Hydrog. Energy* 33, 16068 (2018).
12. A.H. Bhat, T.A. Rangreez, and H.T.N. Chisti, Wastewater treatment and biomedical applications of montmorillonite based nanocomposites: a review. *Curr. Anal. Chem.* 18, 269 (2022).
13. X. Tian, H. Yu, J. Yang, X. Zhang, M. Zhao, Y. Yang, W. Sun, Y. Wei, Y. Zhang, J. Wang, and Z. Ma, Preparation of reverse osmosis membrane with high permselectivity and anti-biofouling properties for desalination. *J. Front. Environ Sci. Eng.* 16, 89 (2022).
14. L. Qalyoubi, A. Al-Othman, and S. Al-Asheh, Recent progress and challenges of adsorptive for the removal of pollutants from wastewater. Part II: environmental applications. *Case Stud. Chem. Environ. Eng.* 3, 100102 (2021).
15. N. Avagimova, G. Polotskaya, N. Saprykina, A. Toikka, and Z. Peintka, Mixed matrix membranes based on polyamide/montmorillonite for pervaporation of methanol-toluene mixture. *Sep. Sci. Technol.* 48, 2513 (2013).
16. P. Natarajan, B. Sasikumar, S. Elakkiya, G. Arthanareeswaran, A.F. Ismail, W. Youravong, and E. Yuliwati, Pillared cloisite 15A as an enhancement filler in polysulfone mixed matrix membranes for CO_2/N_2 and O_2/N_2 gas separation. *J. Nat. Gas. Sci. Eng.* 86, 103720 (2021).
17. M. Purwanto, L. Atmaja, M.A. Mohamed, M.T. Salleh, J. Jaafar, A.F. Ismail, M. Santoso, and N. Widiastuti, Biopolymer-based electrolyte membranes from chitosan incorporated with montmorillonite-crosslinked GPTMS for direct methanol fuel cells. *Rcs. Adv.* 6, 2314 (2016).
18. F. Altaf, R. Batool, R. Gill, Z. Ur Rehman, H. Majeed, A. Ahmad, M. Shafiq, D. Dastan, G. Abbas, and K. Jacob, Synthesis and electrochemical investigations of ABPBI grafted montmorillonite based polymer electrolyte for PEMFC applications. *Renew. Energy* 164, 709 (2021).
19. M.J. Koh, H.Y. Hwang, D.J. Kim, H.J. Kim, Y.T. Hong, and S.Y. Nam, Preparation and characterization of porous PVdF-HFP/clay nanocomposite membranes. *J. Mater. Sci. Technol.* 196, 633 (2011).
20. M. Deka and A. Kumar, Electrical and electrochemical studies of poly(vinylidiene fluoride)-clay nanocomposite gel polymer electrolytes for li-ion batteries. *J. Power Sources* 196, 1358 (2011).
21. J. Kalaiselvimary, K. Selvakumar, S. Rajendran, G. Sowmya, and M.R. Prabhu, Effect of surface-modifued montmorillonite incorporated biopolymer membranes for PEM fuel cell applications. *Polym. Compos.* 40, E301 (2019).
22. K.S. Kumar, S. Rajendran, and M.R. Prabhu, A study of influence on sulfonated TiO_2-poly(Vinylidene fluoride-co-hexafluoropropylene) nano composite membranes for PEM fuel cell application. *Appl. Surf. Sci.* 418, 64 (2017).
23. M.T. Musa, N. Shaari, and S.K. Kamarudin, Carbon nanotube, graphene oxide and montmorillonite as conductive fillers in polymer electrolyte membrane for fuel cell: an overview. *Int. J. Energy Res.* 45, 1309 (2021).
24. V. Yousefi, D. Mohebbi-Kalhori, and A. Samimi, Start-up investigation of the self-assembled chitosan/montmorillonite nanocomposite over the ceramic support as a low-cost membrane for microbial fuel cell application. *Int. J. Hydrog. Energy* 45, 4804 (2020).
25. M. Purwanto, N. Widiastuti, and A. Gunawan, Preparation and properties of chitosan/montmorillonite supported phosphotungstic acid composite membrane for direct methanol fuel cell application. *Korean J. Mater. Res.* 31, 375 (2021).
26. M.L. Para, D. Versaci, J. Amici, M.F. Caballero, M.V. Cozzarin, C. Francia, S. Bodoardo, and M. Gamba, Synthesis and characterization of montmorillonite/polyaniline composites and its usage to modify a commercial separator. *J. Electroanal. Chem.* 880, 114876 (2021).
27. X.W. Wu, N. Wu, C.Q. Shi, Z.Y. Zheng, and H.B. Qi, Proton conductive montmorillonite-Nafion composite membranes for direct ethanol fuel cells. *Appl. Surf. Sci.* 388, 239 (2016).
28. M. Gierszewska, E. Jakubowska, and E. Olewnik-Kruszkowska, Effect of chemical crosslinking on properties of chitosan montmorillonite composites. *Polym. Test.* 77, 105872 (2019).
29. K. Charradi, Z. Ahmed, P. Aranda, and R. Chtourou, Silica/montmorillonite nanoarchitectures and layered double hydroxide SPEEK based composite membranes for fuel cells applications. *Appl. Clay Sci.* 174, 77 (2019).
30. W. Mabrouk, K. Charradi, H.M. Meherzi, A. Alhussein, and S.M.A.S. Keskh, Proton conductivity amelioration of sulfonated poly ether sulfone octyl sulfonamide via the incorporation of montmorillonite. *J. Electro. Mater.* 51, 6369 (2022).
31. M.H. Gouda, T.M. Tamer, A.H. Konsowa, H.A. Farag, and M.S.M. Zldin, Organic/inorganic novel green cation exchange membranes for direct methanol fuel cells. *Energies* 14, 4686 (2021).
32. C.Y. Wong, W.Y. Wong, K.S. Loh, W.R.W. Daud, K.L. Lim, M. Khalid, and R. Walvekar, Development of poly(Vinyl Alcohol)-based polymers as proton exchange membranes and challenges in fuel cell application: a review. *Polym. Rev.* 60, 171 (2020).
33. A.K. Sainul, R. Kannan, P.P. Bahavan, and S. Rajashabala, Role of structural modifications of montmorillonite, electrical properties effect, physical behavior of nanocomposite proton conducting membranes for direct methanol fuel cell applications. *Mater. Sci.* 35, 707 (2017).
34. X. Liao, L. Ren, D. Chen, X. Liu, and H. Zhang, Nanocomposite membranes based on quaternized polysulfone and functionalized montmorillonite for anion-exchange membranes. *J. Power Sources* 286, 258 (2015).
35. F. Ublekov, H. Penchev, V. Georgiev, L. Radev, and V. Sinigersky, Protonated montmorillonite as a highly effective proton-conductivity enhancer in p-PBI membranes for PEM fuel cells. *Mater. Lett.* 135, 5 (2014).
36. K.S. Abidin, R. Kannan, P.P. Palani, and S. Rajashabala, Role of structural modifications of montmorillonite, electrical properties effect, physical behavior of nanocomposite proton conducting membranes for direct methanol fuel cell applications. *Mater. Sci. Poland* 35, 707 (2017).
37. W. Mabrouk, L. Ogier, S. Vidal, C. Sollogoub, F. Matoussi, and J.F. Fauvarque, Ion exchange membranes based upon crosslinked sulfonated polyethersulfone for electrochemical applications. *J. Membr. Sci.* 452, 263 (2014).
38. W. Mabrouk, R. Lafi, K. Charradi, L. Ogier, A. Hafiane, J.F. Fauvarque, and C. Sollogoub, Synthesis and characterization of new proton exchange membrane deriving sulfonated polyether sulfone

using ionic crosslinking electrodialysis applications. *Polym. Eng. Sci.* 60, 3149 (2020).
39. W. Mabrouk, K. Charradi, R. Lafi, H.S. AlSalem, H. Maghraoui-Meherzi, and S.M.A.S. Keshk, Augmentation in proton conductivity of sulfonated polyether sulfone octyl sulfonamide using sepiolite clay. *J. Mater Sci.* 57, 15331 (2022).
40. W. Mabrouk, R. Lafi, J.F. Fauvarque, A. Hafiane, and C. Sollogoub, New ion exchange membrane derived from sulfochlorated polyether sulfone for electrodialysis desalination of brackish water. *Polym. Adv. Technol.* 32, 304 (2021).
41. Z. Ahmed, K. Charradi, Q.A. Alsulami, S.M.A.S. Keshk, and R. Chtourou, Phyysicochemical characterization of low sulfonated polyether ether ketone/Smectite clay composite for proton exchange membrane fuel cells. *J. Appl. Polym. Sci.* 138, 49634 (2021).